J of Nuclear Medicine Technology, first published online November 8, 2021 as doi:10.2967/jnmt.121.262799

18F-DCFPyL PET/CT in Metastatic Renal Cell Carcinoma

Geoffrey M Currie[1], Marko Trifunovic[2], Jui Liu[2], Sang Kim[3] and Howard Gurney[3]

[1]Faculty of Science, Charles Sturt University, Wagga Wagga, Australia

[2]Macquarie Medical Imaging, Macquarie University Hospital, Sydney, Australia

[3]Medical Oncology, Macquarie University, Sydney, Australia

Disclaimer: N/A

Word count: 1400

Corresponding author:
Geoff Currie
School of Dentistry and Health Sciences
Locked Bag 588
Charles Sturt University, Wagga Wagga 2678, Australia
Telephone: 61 2 69332822
Email: gcurrie@csu.edu.au

Key words: 18F-DCFPyL, PET/CT, RCC, metastases

Footline: 18F-DCFPyL in metastatic RCC

Graphical Abstract

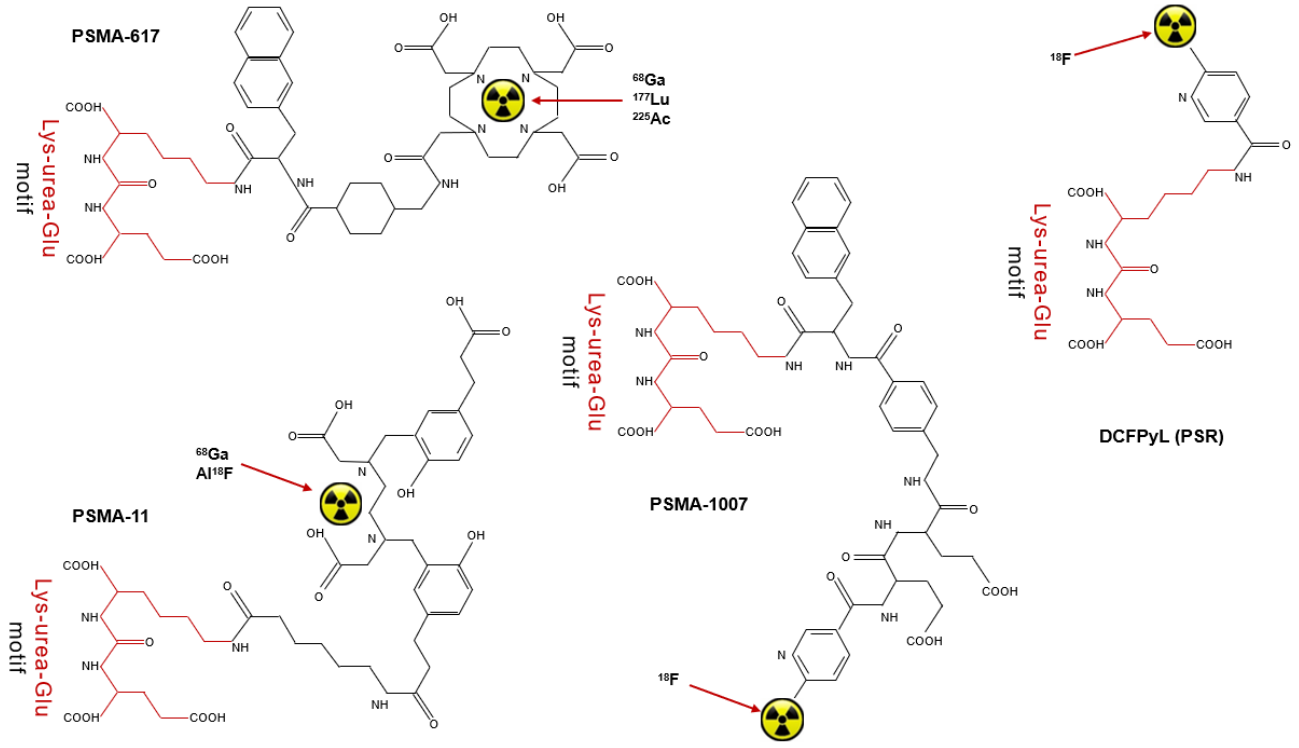

Abstract

Targeted molecular imaging with positron emission tomography (PET) utilize chemical ligands is a peptide that specifically targets a receptor of interest. Prostate specific membrane antigen (PSMA) is substantially upregulated in prostate cancer but is also expressed in the neovascular tissue of several malignancies, including renal cell carcinoma (RCC). Radiolabeled peptide targets for PSMA may be helpful in detecting metastatic RCC lesions. This teaching case provides an insight incidental detection of RCC metastatic disease with PSMA targeted PET and explores potential in deliberate evaluation of RCC with PSMA targeted tracers.

Introduction

Targeted molecular imaging has a foundation in the receptor principle. An important cell surface receptor is the class II membrane glycoprotein prostate specific membrane antigen (PSMA). PSMA is the glutamate carboxypeptidase II enzyme that catalyzes N-acetylaspartylglutamate into glutamate and N-acetylaspartate. PSMA is weakly expressed on normal prostate cells but substantially upregulated in prostate cancer, particularly those of higher grade (*1,2*). It is well known that PSMA is also expressed in the neovascular tissue of several malignancies, including renal cell carcinoma (RCC) (*1-3*). PSMA is also expressed in a range of normal tissues including salivary glands, brain, intestines and proximal renal tubule (*3*).

For PSMA radiotracers, PSMA itself is the receptor target not the peptide and, thus, a numerical suffix generally identifies the specific peptide. PSMA-617, PSMA-11, PSMA-1007 and PSMA-I&T are commonly used. These all share the identical Lys-urea-Glu active portion of the peptide that binds to the receptor. ^{68}Ga PSMA PET/CT imaging provides a high tumor-to-background ratio so has become increasingly important in the detection and localization of prostate cancer. ^{68}Ga is conveniently available via a ^{68}Germanium/^{68}Gallium (^{68}Ge/^{68}Ga) generator that typically services a department for 6-12 months before renewal. ^{18}F PSMA takes advantage of the longer half life of 110 minutes and direct labelling (or Al-F chelation). ^{18}F PSMA is accessible to those without the workload to justify a ^{68}Ga generator and those without an onsite cyclotron. Two versions are most widely reported in the literature; ^{18}F DCFPyL and ^{18}F PSMA-1007. ^{18}F PSMA-1007 has been reported, compared to ^{68}Ga PSMA-11, to have less urinary excretion and bladder visualization and therefore more useful in imaging the prostate bed (*4,5*). 2-(3-{1-carboxy-5-[(6-

[18F]fluoro-pyridine-3-carbonyl)-amino]-pentyl}-ureido)-pentanedioic acid (^{18}F DCFPyL) or dichlorofluorescein (DCF) pyrrolysine (PyL) is widely referred to as PSR or prostate specific radiopharmaceutical. PSR has been reported to have less liver accumulation which may be helpful in detecting liver metastases although higher distribution of dose to the kidneys and lacrimal glands was also noted (*6*). Importantly, PSR has been reported to have higher accumulation than other PSMA probes in lower PSA disease (*6*).

Case

A 70 year old female presented following previous laparoscopic left nephrectomy for clear cell RCC 20 years ago with hematuria and was found to have a bladder mass on imaging. The patient had cystoscopic surgical resection of the bladder mass and histopathology confirmed metastatic clear cell RCC. The patient was referred for a staging ^{18}F DCFPyL PET/CT. 275MBq of ^{18}F DCFPyL was administered intravenously with whole body (vertex to thighs) PET and low dose CT performed 90 minutes after administration.

The ^{18}F DCFPyL PET/CT findings revealed (figure 1) no residual disease in the pelvis and abdomen. There was, however, focal accumulation of ^{18}F DCFPyL (SUV_{max}=7.0) in the left parietal lobe that exhibited a photopenic core and a mild focus (SUV_{max}=2.3) in the right occipital lobe. There was ^{18}F DCFPyL uptake (SUV_{max}=6.2) associated with a large (4.2 x 4.7 x 5.7 cm) soft tissue density mass extending from the inferior pole of the right thyroid lobe distally into the high mediastinum. There was ^{18}F DCFPyL uptake associated with the mediastinal lymph nodes including the right paratracheal (SUV_{max}=4.9), prevascular (SUV_{max}=6.7), and subcarinal (SUV_{max}=5.1) regions. There was also ^{18}F DCFPyL uptake (SUV_{max}=6.7) associated with the left hilar node. Physiologic ^{18}F DCFPyL uptake was noted in the left parotid and bilateral submandibular glands while the right parotid gland was absent (confirmed on co-registered CT).

The ^{18}F DCFPyL PET/CT findings are suggestive of moderate ^{18}F DCFPyL avid cerebral metastases involving the left parietal and right occipital lobes, and lymph nodal metastases involving the mediastinal and the left hilar nodes (figure 2). Moderate ^{18}F DCFPyL avid right thyroid mass may represent thyroid malignancy or further metastatic disease (figure 3). The patient was asymptomatic for both the brain metastases and the mediastinal and hilar nodes.

Follow-up MRI confirmed two brain metastases correlating with the PET/CT. The patient had surgical resection of the brain metastases and histopathology confirmed metastatic clear cell RCC. She then received stereotactic radiosurgery to the surgery bed. A CT scan 2 months later showed progression in mediastinal nodes and thyroid while MRI brain showed resolution of the brain metastases. The patient has started on systemic therapy using lenvatinib and pembrolizumab plus a CTLA4 antibody, on clinical trial. The patient reported thyroid surgery some 30 years prior for a hemorrhagic cyst but no details could be provided.

Discussion

RCC is the most common primary malignancy of the kidney with as many as 35% of patients presenting at the time of diagnosis with metastatic disease (*7*). Clear cell RCC represents 75% of cases and has been targeted with PSMA imaging due to high level of neovascularity and high degree of PSMA expression (*7*). Anatomical characterisation (x-ray, CT and MRI) of metastatic RCC and molecular characterisation with 18F FDG PET are sub-optimal due to their non-specific nature which has further increased interest in PSMA imaging (*7*). PSMA is particularly helpful in detecting small metastatic lesions although study sizes are small. For example, one of the larger studies included 22 RCC patients, 20 with clear cell RCC, and showed patient management was changed from the initial CT staging in 13 of 20 patients using 68Ga-PSMA (*8*). Using PSR, Rowe et al (*9*) evaluated 5 clear cell RCC patients with 18 lesions characterized by conventional imaging and 28 on PSR PET.

Brain metastases are present in 6.5% of RCC patients at the time of diagnosis (*10*) although reports range from 4% to 48% (*11*). Brain metastases are asymptomatic in patients with known RCC metastases in as many as 33% of cases (*11*). The presence of brain metastases is an indicator of poor prognosis (*12*). Given PSMA expression in RCC metastases, the detection of brain metastases in this patient was unexpected but not surprising.

Under normal conditions, both the lacrimal glands and the salivary glands accumulate PSMA targeted radiopharmaceuticals at a high level (*13,14*). Indeed, decreased uptake of PSMA targeted radiopharmaceuticals is a marker for abnormality and this includes under inflammatory conditions (*14*). In this patient, despite normal ^{18}F DCFPyL in salivary glands, the right parotid

salivary gland has an absence of uptake. Careful revision of the low dose non-diagnostic CT (figure 4) suggests an absence of the right parotid gland with replacement of fat tissue. This may reflect the patients vague history of previous surgery associated with a hemorrhagic cyst presumed to be thyroid but may have been mistaken for salivary gland.

Among 12 published articles reporting incidental accumulation of PSMA targeted radiopharmaceuticals in the thyroid, 6 of 23 cases were malignant and 17 of 23 were benign (*15*). Sagar et al (*16*) reported two incidental cases of ^{68}Ga-PSMA uptake in thyroid; the first with extensive accumulation associated with follicular thyroid carcinoma and the second with mild focal accumulation in a thyroid nodule. ^{68}Ga-PSMA imaging was suggested to be of potential value in distinguishing follicular thyroid lesions and at a minimum it is important to be aware of potential thyroid incidentaloma to avoid misinterpretation. Verburg et al (*17*) and Santhanam et al (*18*) have each suggested for anti-PSMA and DCFPyL respectively that PSMA expression offered a potential novel theranostic pair for advanced differentiated thyroid cancer in patients with negative radio-iodine imaging or ^{131}I resistance.

While PSMA targeting PET tracers are well-established in prostate cancer, they have recently been reported to change management in 42% of patients (*19*). Physiological uptake in parenchyma renders PSMA targeted tracers less than ideal for primary RCC, yet it may be useful for detecting metastatic disease (*20*).

Conclusion

PSMA targeting PET tracers provide a useful tool for both incidental and deliberate detection of metastatic RCC and may be particularly useful in the evaluation of small lesions and those in the brain. Further clinical evaluation is recommended to explore efficacy and the potential for theranostic pair approaches to patient management. The availability / affordability of ^{18}F-PSR provides access to PSMA targeted PET imaging at sites without a ^{68}Ge/^{68}Ga generator or onsite cyclotron.

KEY POINTS

QUESTION: Is ^{18}F DCFPyL useful in the evaluation of RCC metastatic disease?

PERTINENT FINDINGS: This case highlights the value of the recently FDA approved ^{18}F DCFPyL for detecting metastatic RCC.

IMPLICATIONS FOR PATIENT CARE: While ^{18}F DCFPyL is valuable in the armamentarium for evaluation of prostate cancer, it also has a potential role to play in RCC and other metastatic disease that exhibits over-expression of PSA.

REFERENCES

1. Bravaccini S, Puccetti M, Bocchini M et al. PSMA expression: a potential ally for the pathologist in prostate cancer diagnosis. *Sci Rep*. 2018:8;4254.
2. Ha H, Kwon H, Lim T, Jang J, Park SK, Byun Y. Inhibitors of prostate-specific membrane antigen in the diagnosis and therapy of metastatic prostate cancer - a review of patent literature. *Expert Opin Ther Pat*. 2021 April 16;1-23. doi: 10.1080/13543776.2021.1878145. Epub ahead of print. PMID: 33459068.
3. Pozzesseren C, Bassanelli M, Ceribelli A et al. Renal Cell Carcinoma: the Oncologist Asks, Can PSMA PET/CT Answer? *Current Urology Reports*. 2019;20:68.
4. Ilhan H, la Fougère C, & Krause BJ. PSMA-based theranostics in prostate cancer. *Urologist*. 2020;59:617-625.
5. Kesch C, Kratochwil C, Mier W, Klaus K, Giesel FL. Gallium-68 or Fluorine-18 for prostate cancer imaging? *Journal of Nuclear Medicine*. 2017;58:687-688.
6. Werner RA, Derlin T, Lapa C, et al. 18F-Labeled, PSMA-Targeted Radiotracers: Leveraging the Advantages of Radiofluorination for Prostate Cancer Molecular Imaging. *Review*. 2020;10:1-16.
7. Yin Y, Campbell S, Markowski M, et al. Inconsistent detection of sites of metastatic non-clear cell renal carcinoma with PSMA-targeted 18F-DCFPyL PET/CT. *Mol. Imaging Biol*. 2019;21:567–573.
8. Siva S, Callahan J, Pryor D, et al. Utility of 68Ga prostate specific membrane antigen positron emission tomography in diagnosis and response assessment of recurrent renal cell carcinoma. J*. Med. Imaging Radiat. Oncol*. 2017;61:372–378.
9. Rowe S, Gorin M, Hammers H, et al. Imaging of metastatic clear cell renal carcinoma with PSMA-targeted 18F-DCFPyL PET/CT. *Ann. Nucl. Med*. 2015;29:877–882.
10. Ke Z, Chen S, Chen Y, et al. Risk Factors for Brain Metastases in Patients with Renal Cell Carcinoma, *BioMed Research International*. 2020; https://doi.org/10.1155/2020/6836234
11. Remon J, Lianes P, Martínez S. Brain metastases from renal cell carcinoma. Should we change the current standard?. *Cancer Treatment Reviews*. 2012;38:249-257.
12. Dudani S, de Velasco G, Wells JC et al. Evaluation of clear cell, papillary, and chromophobe renal cell carcinoma sites and association with survival. *JAMA Network Open*. 2021;4(1):e2021869.
13. van Kalmthout L, Lam M, de Keizer B, et al. Impact of external cooling with icepacks on 68Ga-PSMA uptake in salivary glands. *EJNMMI Research*. 2018;8:56.
14. Rupp N, Umbricht CA, Pizzuto DA, et al. First clinicopathological evidence of a non PSMA-related uptake mechanism for (68)Ga-PSMA-11 in salivary glands. *Journal of Nuclear Medicine*. 2019;60:1270–1276.
15. Bertagna F, Albano D, Giovanella L, Bonacina M, Durmo R, Giubbini R, Treglia G. 68Ga-PSMA PET thyroid incidentalomas. *Hormones (Athens)*. 2019;18:145-149.
16. Sager S, Vatankulu B, Uslu L, Sönmezoglu K. Incidental Detection of Follicular Thyroid Carcinoma in 68Ga-PSMA PET/CT Imaging. *J Nucl Med Technol*. 2016;44:199-200.

17. Verburg FA, Krohn T, Heinzel A, Mottaghy FM, Behrendt FF. First evidence of PSMA expression in differentiated thyroid cancer using [68Ga]PSMA-HBED-CC PET/CT. *Eur J Nucl Med Mol Imaging*. 2015;42:1622–1623.

18. Santhanam P, Russell J, Rooper LM, et al. The prostate-specific membrane antigen (PSMA)-targeted radiotracer 18F-DCFPyL detects tumor neovasculature in metastatic, advanced, radioiodine-refractory, differentiated thyroid cancer. *Med Oncol*. 2020;37;98.

19. Raveenthiran S, Esler R, Yaxley J, Kyle S. The use of ^{68}Ga-PET/CT PSMA in the staging of primary and suspected recurrent renal cell carcinoma. *Eur J Nucl Med Mol Imaging*. 2019;46:2280-2288.

20. Lindenberg L, Mena E, Choyke P, Bouchelouche K. PET imaging in renal cancer, *Curr Opin Oncol.* 2019;31:216–221.

Figure 1: Representative coronal slices of the ^{18}F DCFPyL PET scan. Physiologic ^{18}F DCFPyL uptake was noted in the left parotid and bilateral submandibular glands while the right parotid gland was absent (A).Focal accumulation of ^{18}F DCFPyL in the left parietal lobe (B). There was ^{18}F DCFPyL uptake associated with the mediastinal lymph nodes (C). There was also ^{18}F DCFPyL uptake associated with the left hilar node (D).

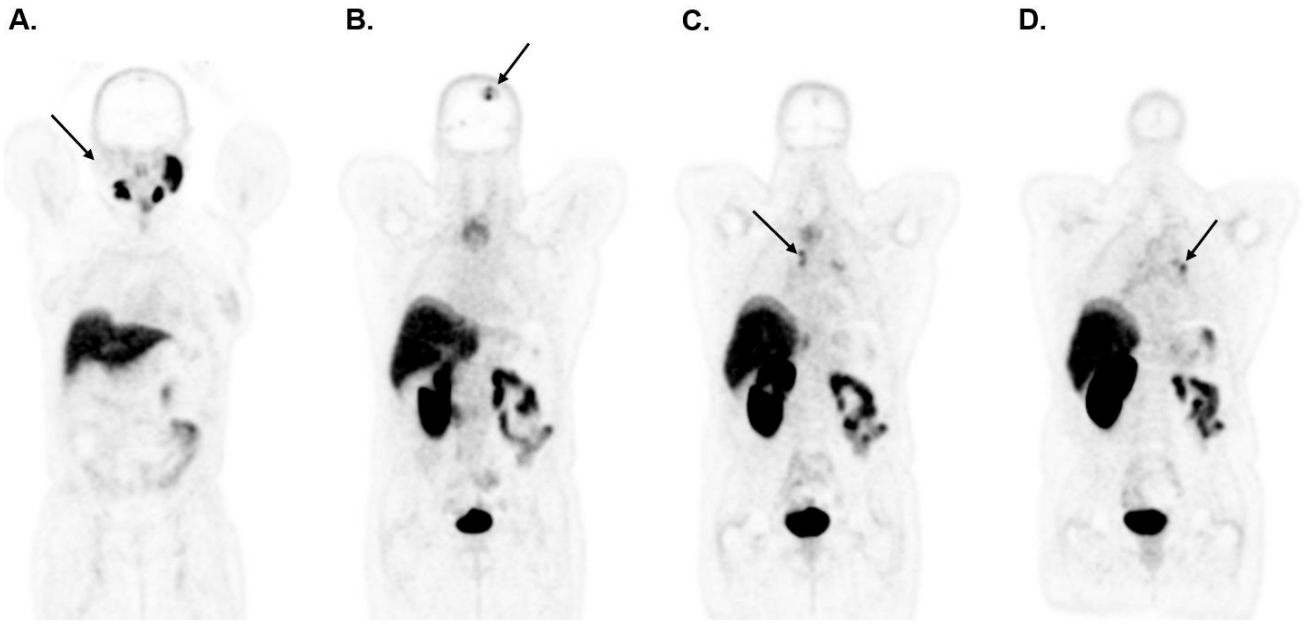

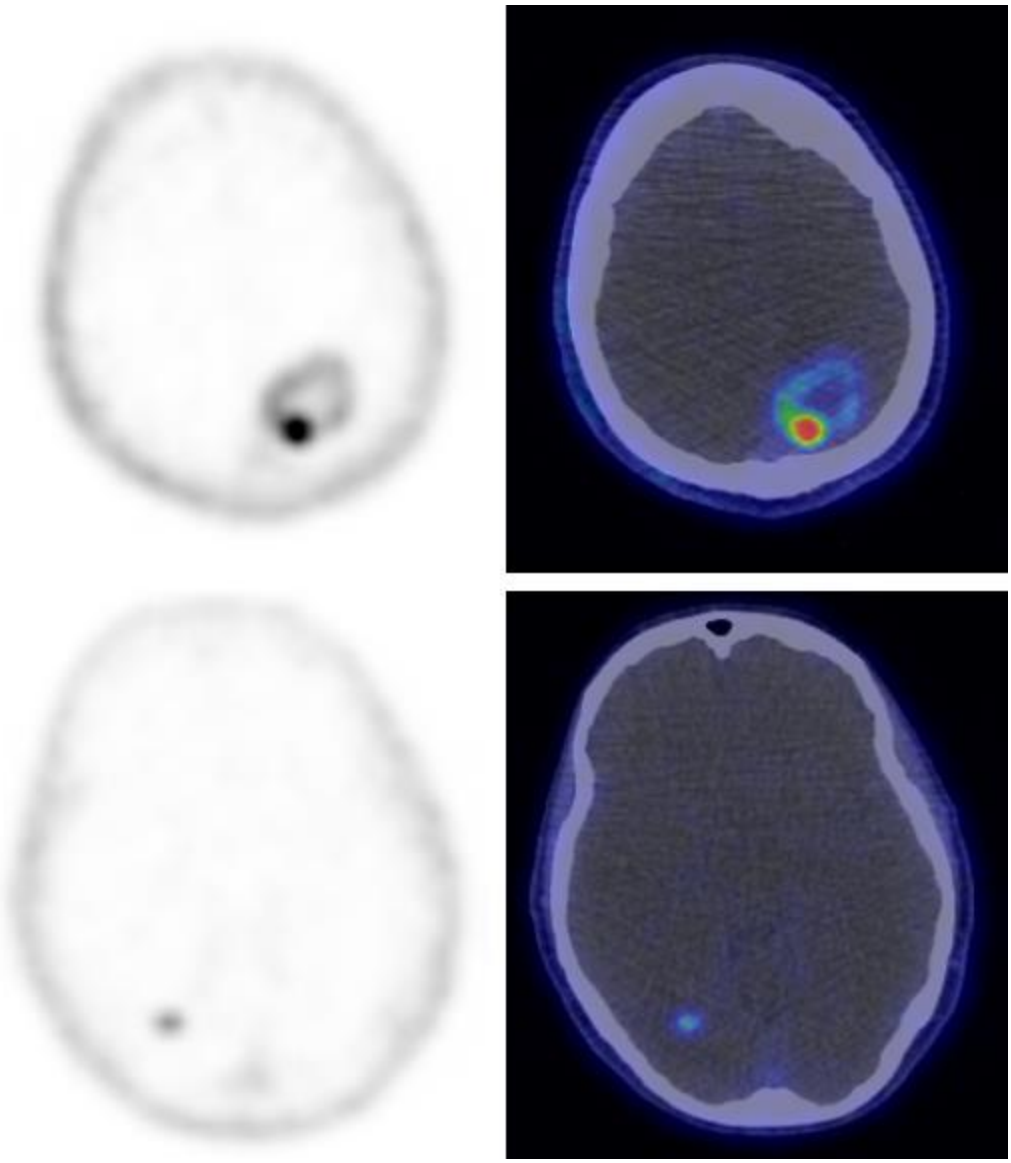

Figure 2: ^{18}F DCFPyL PET scan with transaxial slices through the head demonstrating left parietal and right occipital cerebral metastases.

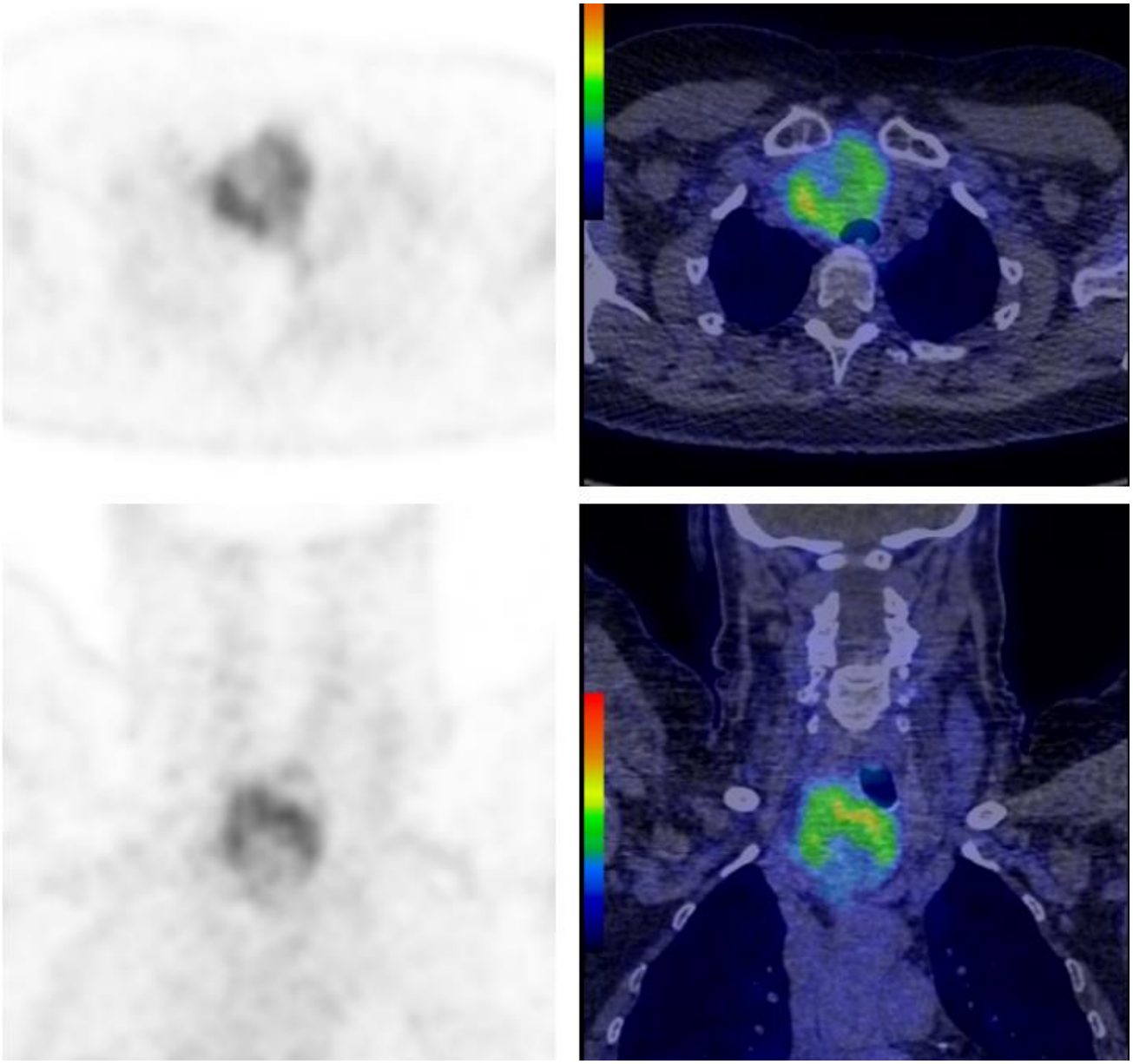

Figure 3: ^{18}F DCFPyL uptake with low dose CT co-registration in the right thyroid lesion.

Figure 4: ^{18}F DCFPyL PET with low dose CT co-registration indicating absent accumulation in the right parotid salivary gland.